

Supplement of Atmos. Meas. Tech., 14, 945–959, 2021
<https://doi.org/10.5194/amt-14-945-2021-supplement>
© Author(s) 2021. This work is distributed under
the Creative Commons Attribution 4.0 License.



Supplement of

Quantifying fugitive gas emissions from an oil sands tailings pond with open-path Fourier transform infrared measurements

Yuan You et al.

Correspondence to: Ralf M. Staebler (ralf.staebler@canada.ca)

The copyright of individual parts of the supplement might differ from the CC BY 4.0 License.

S1. Methane mole fractions, vertical profiles, and gradient fluxes

S1.1 Calibration of retrieved CH₄ mole fraction from OP-FTIR

The amplitude of spectra for all the three paths varied substantially over the study period, especially for the top path. As a proxy for the spectral amplitude, the signal-to-noise ratio (SNR) of the CH₄ fitting was used. The CH₄, NH₃, CH₃OH and HCHO mole fraction for all three paths when this SNR dropped fast, or stayed below 10 were flagged. 3% and 13% of the measurements from bottom and top path were flagged and invalidated from further mole fraction gradient and flux calculations.

Since CH₄ mole fraction was also continuously measured by cavity ring-down spectroscopy (CRDS) at four heights during the study, the measurements at 4m were compared to CH₄ mole fraction retrieved from the FTIR bottom path to calibrate the retrieved CH₄ mole fraction from three paths of this OP-FTIR system.

Each CRDS in this study was calibrated before and after the campaign, and CH₄ mole fraction from three CRDS at the same height was well compared ($r^2 > 0.96$, slope=0.98 - 1.01, intercept = 0.01 - 0.02 ppm). Therefore, CH₄ mole fraction retrieved from FTIR all three paths were calibrated by the linear relationship in Fig. S1:

$$[\text{CH}_4]_{\text{FTIR_calibrated}} = 1.2015 \times [\text{CH}_4]_{\text{FTIR_retrieved}} - 0.397 \quad (\text{S. 1})$$

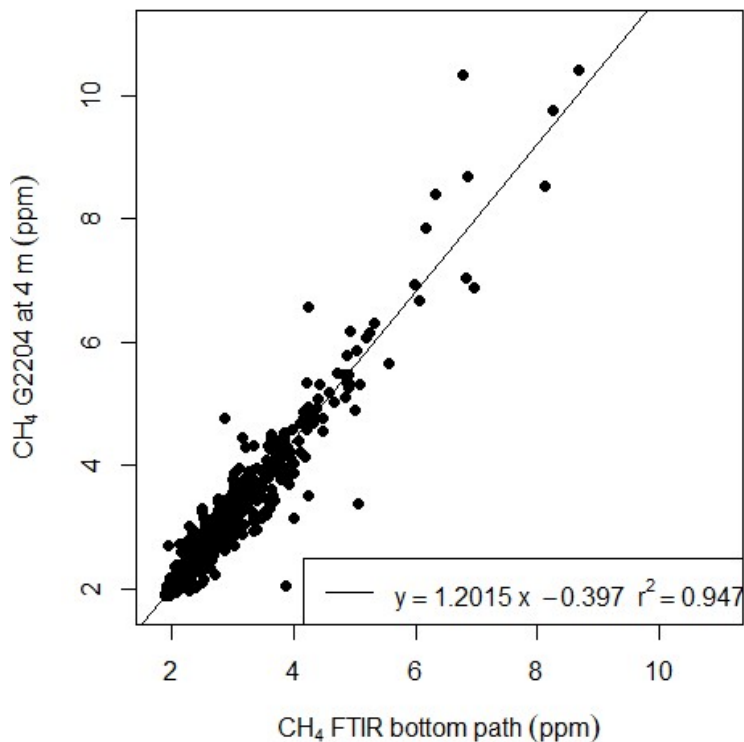


Figure S 1 CH₄ mole fraction retrieved from FTIR bottom path compared to CH₄ mole fraction measured by CRDS (G2204) at 4m. Data are half-hour averaged results.

S1.2 Mole fractions and vertical profiles with gradient fluxes

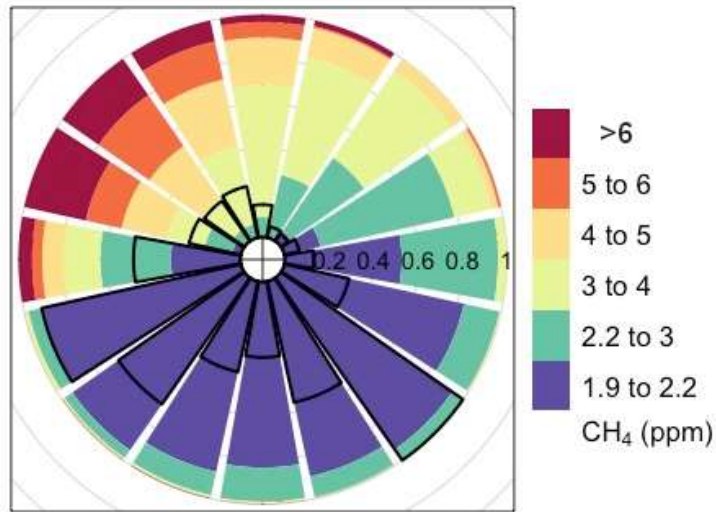


Figure S 2 Normalised rose plot of CH₄ mole fractions from FTIR bottom path. Colors represent CH₄ mole fractions. The length of each colored segment presents the time fractions of that mole fraction in each direction bin. The radius of the black open sectors indicates the frequency of wind in each direction bin; angle represents wind direction: straight up is north and straight left is west.

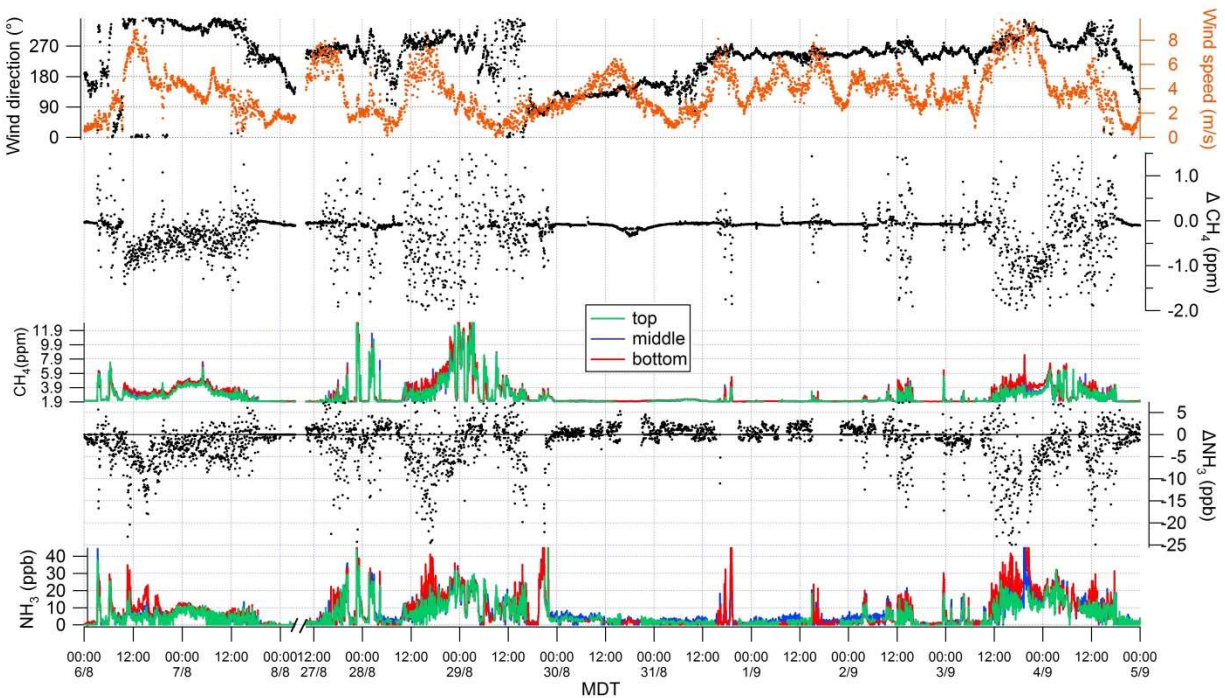


Figure S 3 Time series of wind direction, wind speed, difference in CH₄ mole fractions from the top and bottom paths, CH₄ mole fractions, difference in NH₃ mole fractions from the top and bottom paths, and NH₃ mole fractions, from Aug 6th to 8th, and from Aug 27th to Sept 5th. MDT = mountain daylight savings time.

In the analysis of methane vertical profile below, all the mole fractions measurements (half-hour averages) were taken from the Picarro G2204 at 4, 8, 18, and 32m. There are 271 half-hours in total when the wind was from the pond. About 83% of the half-hour periods when the wind was from the pond direction, the CH₄ vertical profiles are similar to Fig. S4. Within this 83% of periods, some profiles are close to linear, and others are not strict decreasing trend with height. For the rest of 17% of half-hour periods, the CH₄ vertical profiles are closer to logarithmic (Fig. S5). Therefore, CH₄ vertical profiles are considered linear over the entire period for calculating gradient flux with OP-FTIR measurement.

In addition, those half-hour periods when logarithmic relationship is better than linear to describe the vertical profile are mainly (65%) associated with wind speed greater than 6 m s⁻¹ (Fig. S6). For the majority of the time (85%) when the wind was from the pond, wind speed was less than 6 m s⁻¹ (Fig. S6).

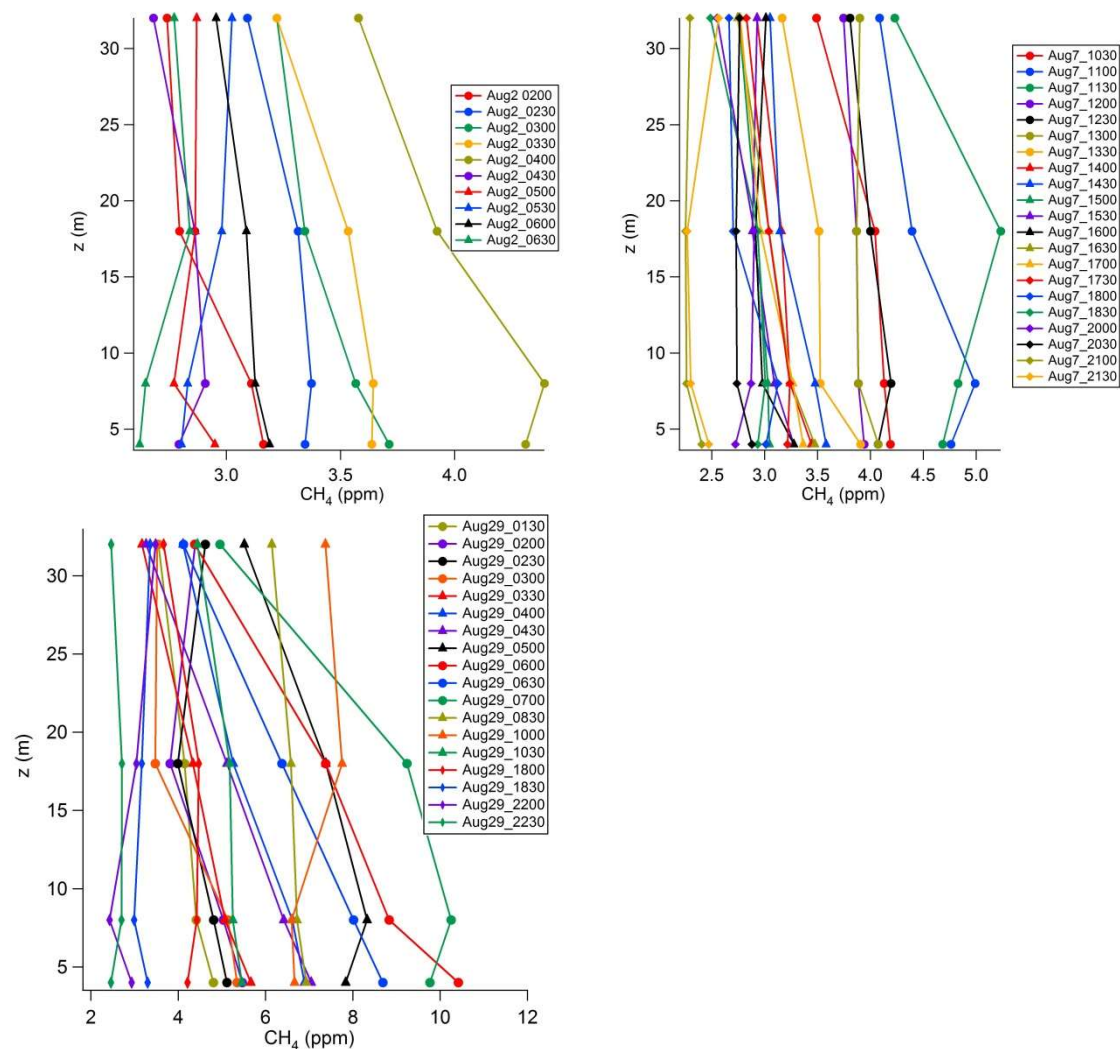


Figure S 4 Examples of observed CH₄ mole fraction vertical profiles, when the profiles are close to linear.

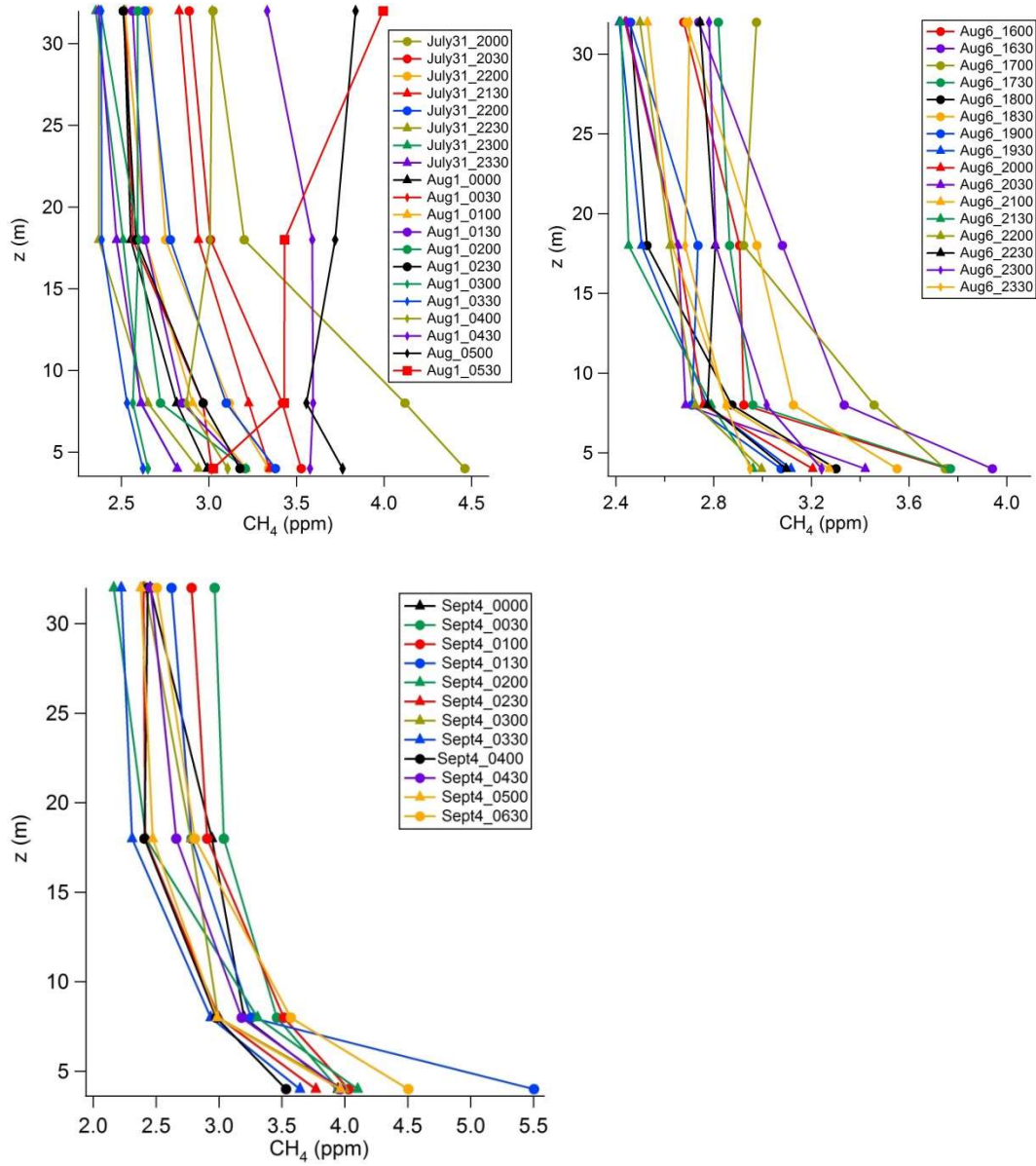


Figure S 5 Examples of observed CH₄ mole fraction vertical profiles, when the profiles are close to logarithmic.

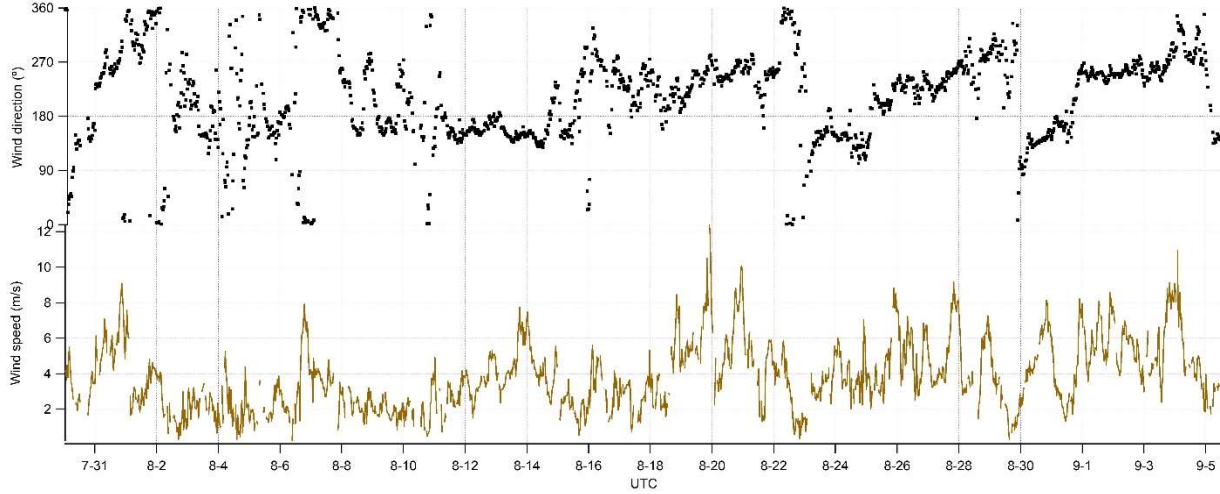


Figure S 6 Time series of wind direction and wind speed measured at 18m over the entire project.

To compare to the assumption of linear vertical profile of CH₄ mole fractions, the calculation of K_c for the assumption of logarithmic vertical profile is also listed here. The representative average height of the FTIR top path with a logarithmic vertical profile would be $Z_{top} = \sqrt{23 \times 1} = 4.8 \text{ m}$. Then, K_c for gradient flux calculated from the top-to-bottom path gradient is adjusted logarithmically based on the $K_{c_{2,4}}$ calculated from point measurements at 8m and 32m on the tower:

$$F_{gradient_{FTIR}} = -K_{c_{FTIR_{log}}} \times \frac{\partial c}{\partial z} = \frac{-K_{c_{FTIR_{log}}} \times \partial c}{z \times \ln\left(\frac{z_2}{z_1}\right)} = -\frac{K_{m_{FTIR_{log}}}}{K_{m_{8,32m}}} \times K_{c_{8,32m}} \times \frac{\partial c}{\sqrt{4.79 \times 1} \times \ln\left(\frac{4.79}{1}\right)} = -0.291 \times \frac{K_{m_{FTIR_{log}}}}{K_{m_{8,32m}}} \times K_{c_{8,32m}} \times \partial c \quad (\text{S. 2}),$$

where z is the height for which flux is calculated (Thompson and Pinker, 1981).

$\frac{K_{m_{FTIR_{log}}}}{K_{m_{8,32m}}}$ is a function of stability (z/L) and is calculated with eq. (5) and (6) in the main text. The gradient flux of CH₄ with logarithmic vertical profile is calculated with eq. (S2) and the area-weighted average flux from the pond sectors is 4.1 gm⁻²d⁻¹, which is 19% greater than the gradient flux calculated with linear vertical profile.

Beside top-bottom paths of CH₄ mole fractions gradient, middle-bottom paths of gradient can also be used to calculate CH₄ gradient fluxes. The results are summarised in the first row of Table S1 to compare to gradient fluxes with top-bottom paths CH₄ gradients. The area-weighted averaged fluxes with middle-bottom paths is 29% lower than the area-weighted averaged fluxes with top-bottom paths (Table S1).

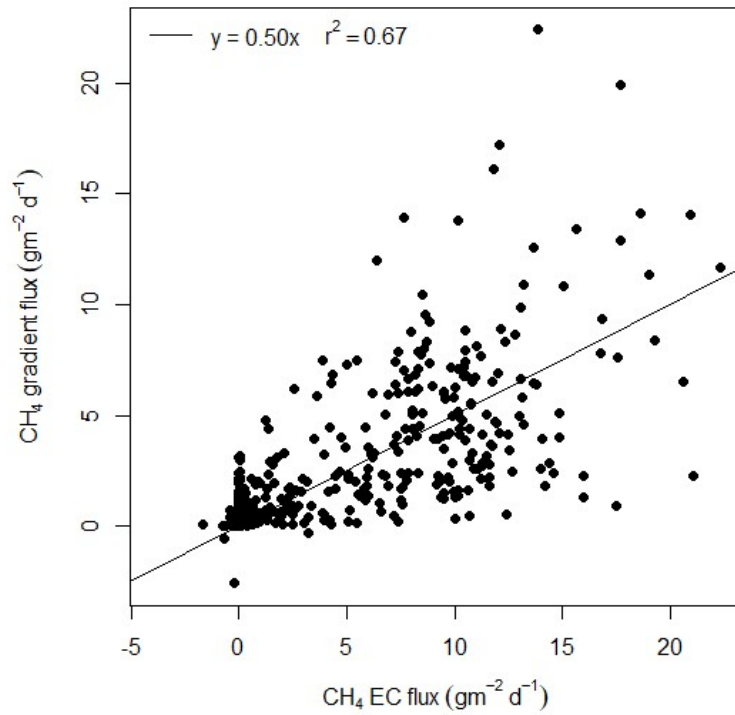


Figure S 7 CH₄ gradient flux from OP- FTIR compared with EC flux.

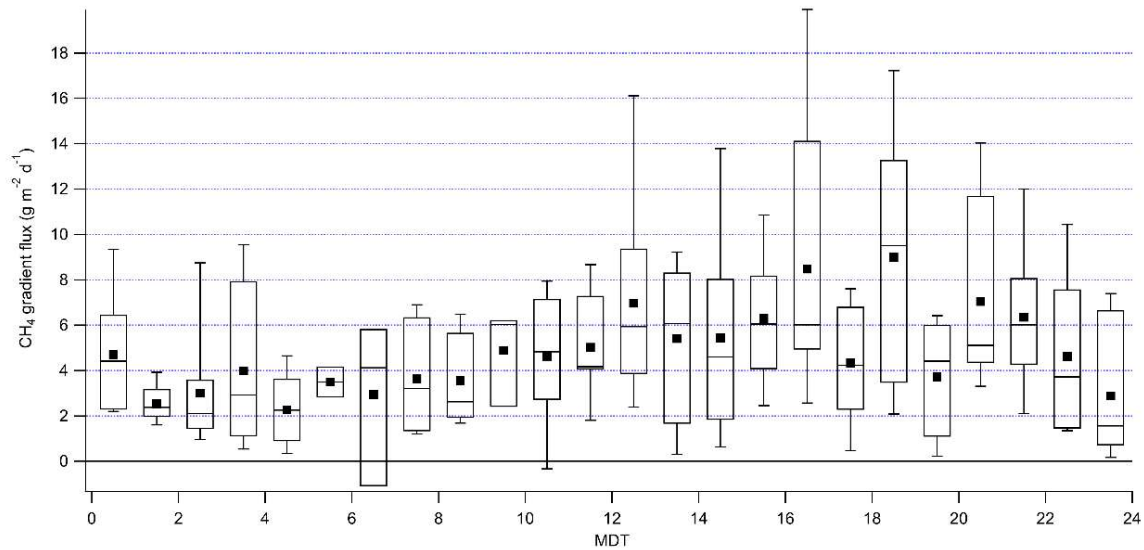


Figure S 8 Diurnal variation of CH₄ gradient flux from FTIR, when the wind came from the pond direction. MDT = mountain daylight savings time. Lower and upper bounds of the box plot are the 25th and 75th percentile; the line in the box marks the median and the black square labels the mean; the whiskers label the 10th and 90th percentile.

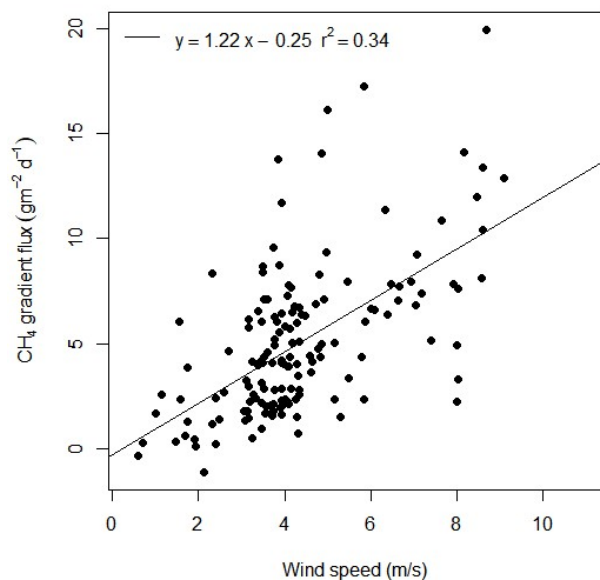


Figure S 9 CH₄ gradient flux when the wind was from the pond.

S1.3 IDM flux of CH₄ with two approaches of determining background mole fraction input

IDM fluxes of CH₄ with input from FTIR. Fluxes comparison with background mole fraction using ECCC measurement at south, and AEP measurements at north:

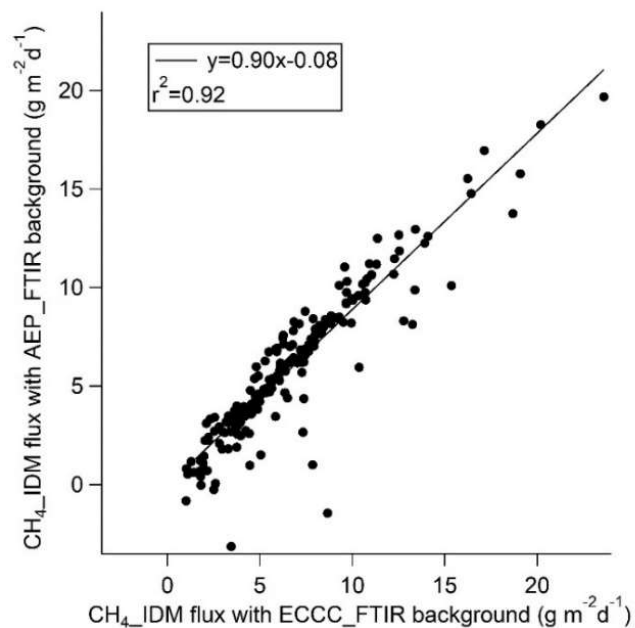


Figure S 10 comparison of CH₄ IDM fluxes with input background mole fraction from the south and north measurements.

The half-hour IDM fluxes with these two approaches agree well (slope = 0.9, $r^2 = 0.92$). The sector-area-weight-averaged IDM fluxes with two approaches are also within 20% difference. The interquartile ranges overlap (Table S1).

S2. NH₃

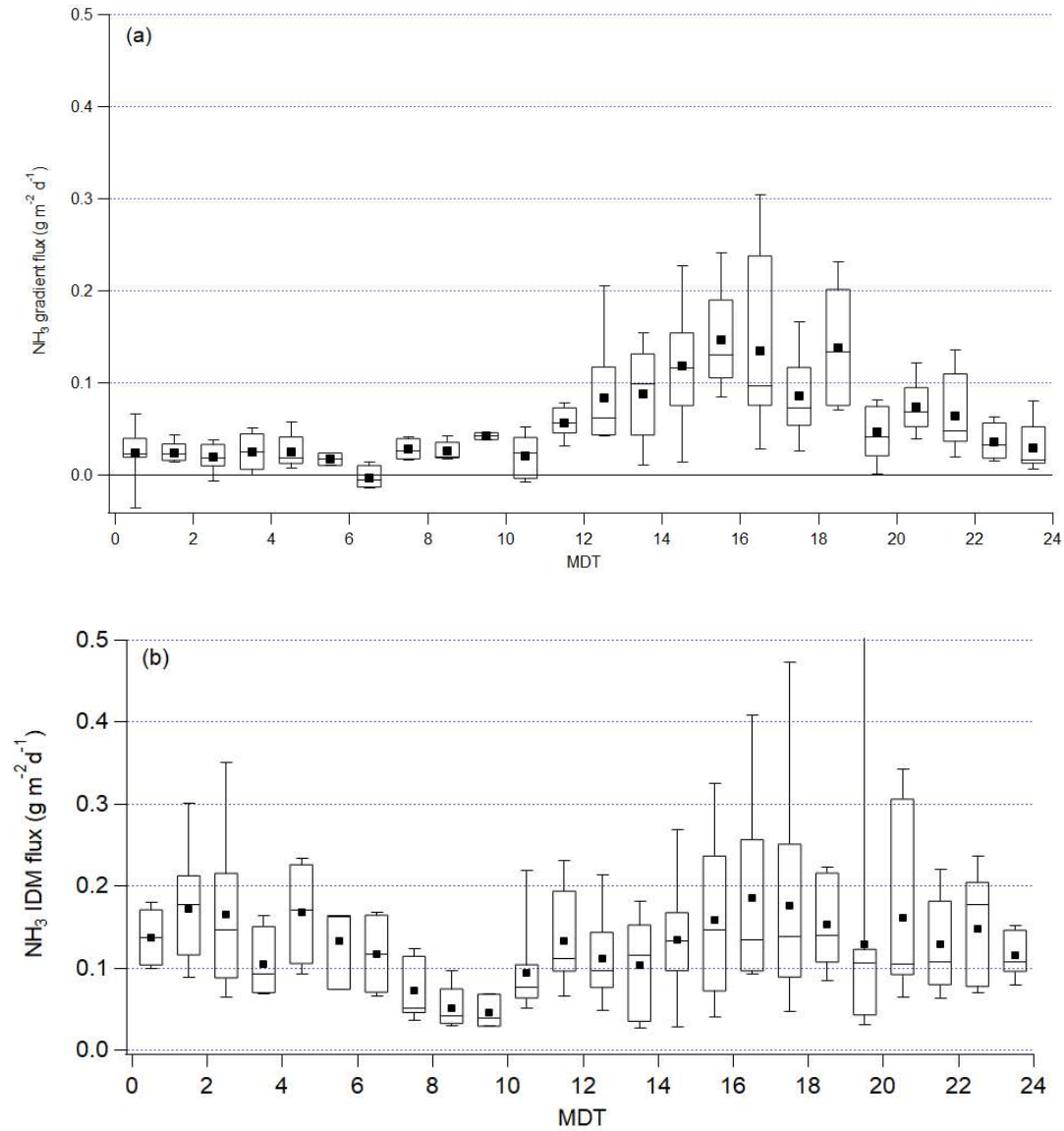


Figure S 11 Diurnal variations of NH₃ gradient flux derived from top-bottom paths (a) and IDM flux (b) when the wind was from the pond direction. MDT = mountain daylight savings time. Lower and upper bounds of the box plot are the 25th and 75th percentile; the line in the box marks the median and the black square labels the mean; the whiskers label the 10th and 90th percentile.

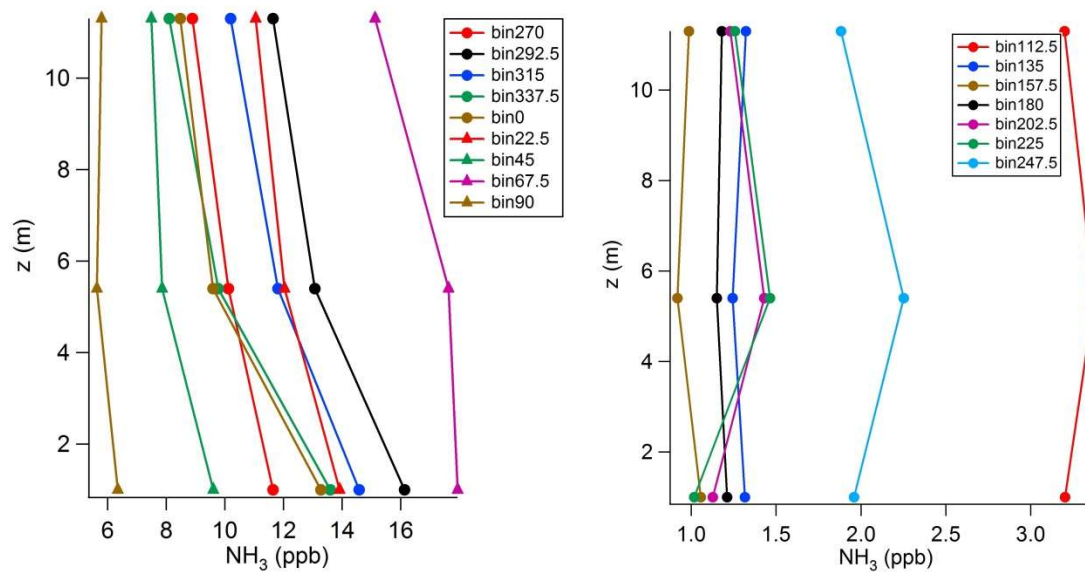


Figure S 12 NH₃ mole fraction vertical profiles after averaging in 16 wind direction sectors. The height z for the three paths are the height of the middle point of each path.

S3. Total alkane

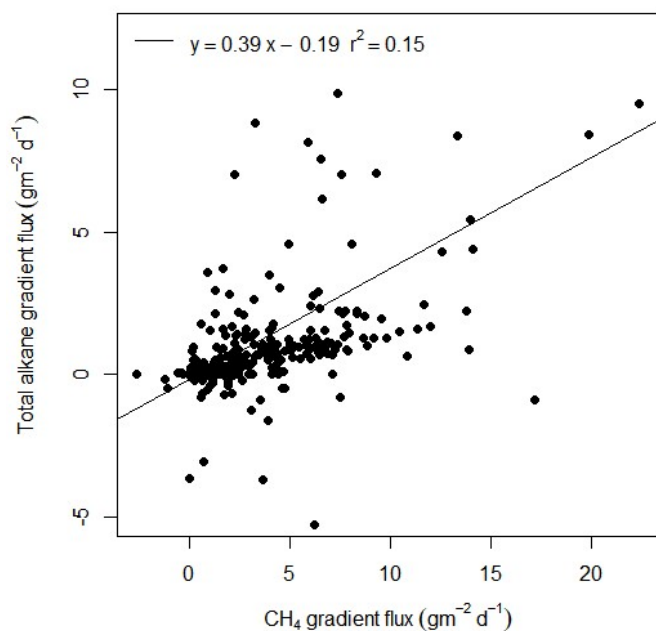


Figure S 13 Total alkane gradient flux compared to CH₄ gradient flux, both derived from OP-FTIR top and bottom paths.

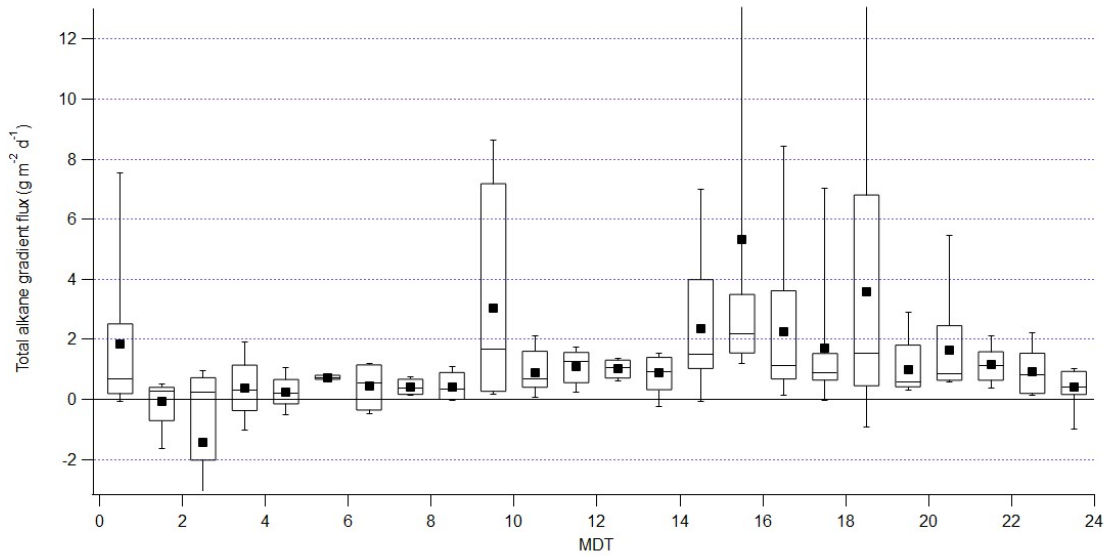


Figure S 14 Diurnal variation of total alkane gradient flux when the wind was from the pond direction. MDT = mountain daylight savings time. Lower and upper bounds of the box plot are the 25th and 75th percentile; the line in the box marks the median and the black square labels the mean; the whiskers label the 10th and 90th percentile.

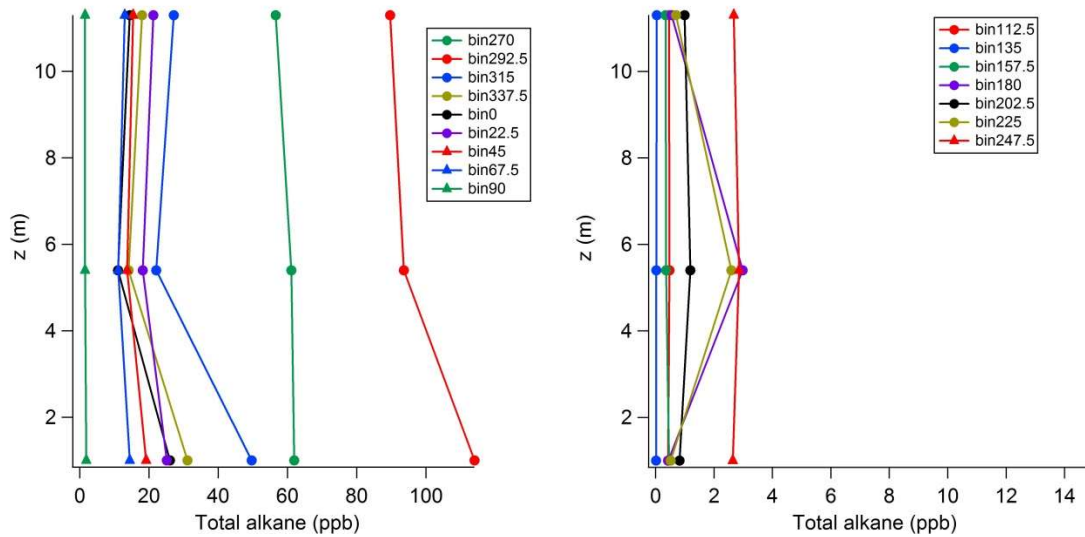


Figure S 15 Total alkane mole fraction vertical profiles after averaging in 16 wind direction sectors. The height z for the three paths are the height of the middle point of each path.

S4. Methanol (CH₃OH)

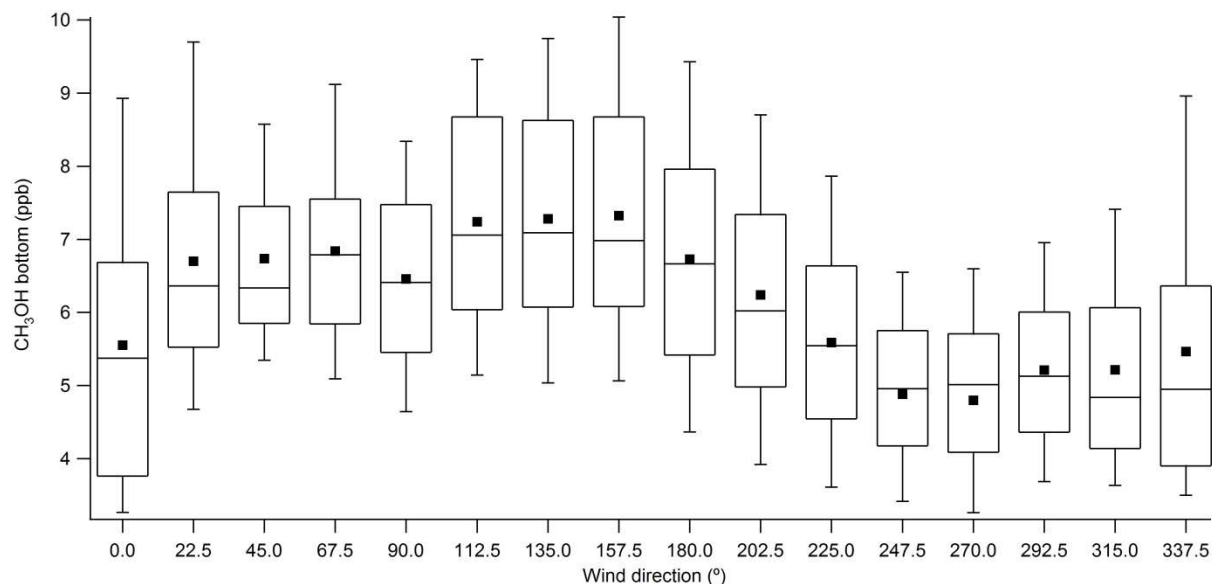


Figure S 16 CH₃OH mole fraction retrieved from the FTIR bottom path, binned in 22.5° sectors. Lower and upper bounds of the box plot are the 25th and 75th percentile; the line in the box marks the median and the black square labels the mean; the whiskers label the 10th and 90th percentile.

S5. Flux results with the slant path approach from Flesch et al. (2016)

As briefly discussed in the introduction of the main text, Flesch et al., (2016) deployed OP-FTIR measurement with “slant path” configuration, and derived emission rates of N₂O and NH₃ by flux-gradient method. To compare the methods we used to calculate gradient fluxes with their approach, we also performed similar calculation. The derived u^* and L directly from sonic anemometer measurement at 8m on the tower, mole fraction difference between top and bottom paths of FTIR, and calculated S_c were plugged in equation (9) in Flesch et al., (2016). In this study, calculated S_c is allowed to vary with dynamic stability (You et al. (2021) Fig. 3), while in Flesch et al. (2016) S_c was a constant 0.64. The time series of half-hour gradient fluxes of CH₄, NH₃ and total alkane were calculated. Area-weight-averaged fluxes were calculated and summarized in Table S1. Compared to gradient flux results with our approach modified Bowen ratio, CH₄, NH₃ and total alkane fluxes with the slant path flux-gradient method are 24%, 25%, and 30% smaller.

Tables

Table S1 Summary of CH₄ IDM fluxes with two background approaches, and gradient fluxes with approach from Flesch et al. (2016).

(g m ⁻² d ⁻¹)	Q_25%	median	Q_75%	mean ^a
CH ₄ gradient flux with middle-bottom paths	1.5	2.6	4.1	3.0 ± 1.3
CH ₄ IDM flux_ with ECCC background	3.6	5.2	6.6	5.4 ± 0.4
CH ₄ IDM flux_ with AEP background	2.9	4.4	5.6	4.3 ± 0.6
CH ₄ gradient flux with approach from Flesch et al. (2016)	1.5	2.9	4.6	3.3 ± 1.3
NH ₃ gradient flux with approach from Flesch et al. (2016)	0.01	0.03	0.06	0.04 ± 0.01
Total alkane gradient flux with approach from Flesch et al. (2016)	0.16	0.50	1.08	0.74 ± 0.15

^a Errors with the mean fluxes are calculated with an integrative approach: the average of observed standard deviations of fluxes from five periods when the fluxes displayed high stationarity.

Reference

Kljun, N., Calanca, P., Rotach, M. W., and Schmid, H. P.: A simple two-dimensional parameterisation for Flux Footprint Prediction (FFP), *Geosci. Model Dev.*, 8, 3695-3713, <http://doi.org/10.5194/gmd-8-3695-2015>, 2015.

Thompson, O. E., and Pinker, R. T.: An error analysis of the Thornthwaite-Holzman equations for estimating sensible and latent heat fluxes over crop and forest canopies, *J. Appl. Meteorol.*, 20, 250-254, 1981.